

# Dynamic Positron Computed Tomography of the Heart with a High Sensitivity Positron Camera and Nitrogen-13 Ammonia

Nagara Tamaki, Michio Senda, Yoshiharu Yonekura, Hideo Saji, Shusei Kodama, Yutaka Konishi, Toshihiko Ban, Hirofumi Kambara, Chuichi Kawai, and Kanji Torizuka

*Departments of Radiology and Nuclear Medicine, Cardiovascular Surgery, and Internal Medicine, Kyoto University School of Medicine, Kyoto, Japan*

Dynamic positron computed tomography (PCT) of the heart was performed with a high-sensitivity, whole-body multislice PCT device and [ $^{13}\text{N}$ ]ammonia. Serial 15-sec dynamic study immediately after i.v. [ $^{13}\text{N}$ ]ammonia injection showed blood pool of the ventricular cavities in the first scan and myocardial images from the third scan in normal cases ( $n = 4$ ). In patients with myocardial infarction ( $n = 8$ ) and mitral valve disease ( $n = 2$ ), tracer washout from the lung and myocardial peak time tended to be longer, suggesting presence of pulmonary congestion. PCT delineated tracer retention in the dorsal part of the lung. Serial 5-min late dynamic study in nine cases showed gradual increase in myocardial activity for 30 min in all normal segments and 42% of infarct segments, while less than 13% activity increase was observed in 50% of infarct segments. Thus, serial dynamic PCT with [ $^{13}\text{N}$ ]ammonia assessing tracer kinetics in the heart and lung is a valuable adjunct to the static myocardial perfusion imaging for evaluation of various cardiac disorders.

J Nucl Med 26:567-575, 1985

Positron computed tomography (PCT) is a valuable imaging technique for evaluation of regional physiological and metabolic process in vivo. PCT offers potential capability of noninvasive measurement of tissue tracer concentration (1,2). PCT of the myocardium permits quantitative measurement of blood perfusion (2-4), fatty acid and glucose metabolism (5,6), uptake of amino acids (7), and infarct volume (8). With the development of recent technology, multislice PCT devices with high performance have appeared (9); however, most of them have been utilized only for brain imaging. We have constructed a whole-body multislice PCT device (10-12). This device, providing seven cross sections simultaneously with high spatial resolution, permits serial dynamic study of various organs in whole-body so

that uptake and turnover of the tracer can be assessed.

We postulated that dynamic cardiac PCT with nitrogen-13 ( $^{13}\text{N}$ ) ammonia could provide additional information on the tracer kinetics. This paper describes the value of serial dynamic PCT of the heart with the multislice PCT device and  $^{13}\text{N}$ -labeled ammonia.

## MATERIALS AND METHODS

### Preparation of [ $^{13}\text{N}$ ]ammonia

Nitrogen-13-labeled ammonia was produced with an ultra-compact cyclotron\* at our institution by water irradiation with 14.5 MeV protons according to  $^{16}\text{O}(p,\alpha)^{13}\text{N}$  reaction and subsequent reaction with titanous hydroxide. The  $^{13}\text{N}$  ammonia thus produced was collected in a saline solution. After correction of acid-base balance, it passed through a Millipore filter. The  $^{13}\text{N}$  preparation was carried out under sterile pyrogen-free condition.

Received Aug. 28, 1984; revision accepted Feb. 27, 1985.

For reprints contact: Yoshiharu Yonekura, MD, Dept. of Radiology & Nuclear Medicine, Kyoto University School of Medicine, Shogoin, Sakyo-ku, Kyoto, 606 Japan.

### PCT device

The PCT camera (Positologica III) had four detector rings with 192 BGO crystals (12 mm × 24 mm × 24 mm) arranged at irregular intervals along each ring, so that seven transverse slices at 16-mm intervals could be obtained simultaneously. Data sampling was performed by continuous rotation of the detectors (10,11). The patient aperture was 54 cm in diam and the field of view was 40 cm in diam and 12 cm in depth. Spatial resolution was 7.6 mm at the center of field in full width at half maximum. The sensitivity for 20-cm-diam cylindrical phantom was 34.2 and 52.5 kcps/ $\mu$ Ci/ml for in-plane and cross-plane, respectively (10,11).

### Patients studies

We studied ten patients with myocardial infarction (MI), two patients with mitral valve disease (MVD), and six normal volunteers (N) as a control group. All of the normal subjects were male, asymptomatic, and without evidence of coronary artery disease by history and electrocardiogram. The ten patients with MI were documented by history of acute onset of chest pain, elevation of cardiac enzymes and change of electrocardiogram, and all were confirmed by contrast angiography. The range of ejection fraction calculated by radionuclide ventriculography was 21 to 64%. Three of them showed decreased ejection fraction (less than 40%). The two patients with MVD were documented with echocardiography and contrast angiography.

Fourteen cases (four N, eight MI, and two MVD) underwent early dynamic scan and nine cases (three N and six MI) received subsequent late dynamic scan.

Each patient was positioned in Positologica III and transmission images of the chest were obtained with continuous rotation of germanium-68/gallium-68 plate source to allow correction of photon attenuation on the emission images. Ten to 20 mCi of [<sup>13</sup>N]ammonia were injected i.v. as a bolus from the antecubital vein. Immediately following the injection, serial 15-sec sampling was performed for 3–5 min as an early dynamic scan. From 3–5 min after injection, serial 5-min sampling was performed for another 30 min as a late dynamic scan. Each tomographic image was displayed as 128 × 128 pixels. More than 400,000 counts were obtained per slice in the early dynamic scan and 3 to 8 million counts were collected per slice in the late dynamic scan.

### Data analysis

Time-activity curves were created from the early dynamic scan by locating three or four regions of interest (ROIs) (2 × 2 pixels) in the left ventricular cavity and myocardium as well as 4 × 4 pixels ROIs in the middle of the lung field, and determining the mean counts within the ROIs after correction of <sup>13</sup>N physical decay.

For quantitative analysis of temporal tracer change in each region, half-time of the lung washout curve (lung- $t_{1/2}$ ) was calculated from the pulmonary activity curve after five-point smoothing of the curve. The time from the injection to the early maximal myocardial activity (myocardial-peak time) was also obtained from the time-activity curve of the myocardium. From the late dynamic scan, counts in regional myocardium at 30 min were calculated as percent increase from the initial value by locating five ROIs in the left ventricular myocardium in each tomographic plane. These quantitative data from corresponding ROIs were averaged from the two central planes of the images.

## RESULTS

### Early dynamic scan

#### Normal case (Fig. 1)

Serial 15-sec dynamic PCT images of a normal case immediately following [<sup>13</sup>N]ammonia injection are shown in Fig. 1a. Blood pool of both ventricles and the aorta was visualized in the first scan, and the left ventricular myocardium was delineated from the third scan. The time-activity curves in the early dynamic scan (Fig. 1b) showed rapid clearance of the blood pool and the lung activities with early peak of the myocardium. The static images at 3 min after injection (Fig. 1c) revealed homogeneous tracer distribution in the left ventricular myocardium.

#### Case with myocardial infarction (Fig. 2)

In rapid serial dynamic PCT images of a case with myocardial infarction (Fig. 2a), ventricular cavities appeared at the first two scans (within 30 sec) and the myocardial activity was obtained from the fifth scan. Prolonged pulmonary activity, especially in the dorsal region was noted, suggesting the presence of pulmonary congestion. The time-activity curves (Fig. 2b) indicated delayed clearance of the lung activity with slow washin into the myocardium. The static images in this case (Fig. 2c) showed myocardial perfusion defect in apical and posterolateral regions with visualization of the right ventricular myocardium. The contrast between the myocardium and lung was decreased as compared to the normal case described in Fig. 1.

#### Case with mitral stenosis (Fig. 3)

In serial 15-sec dynamic PCT images of a case with mitral stenosis (Fig. 3a), blood-pool activity appeared at the first two scans with marked pulmonary activity, especially in the posterior lung, indicating the presence of pulmonary congestion. The time-activity curves in this case (Fig. 3b) indicated delayed washout of the lung activity with gradual increase in the myocardial activity.

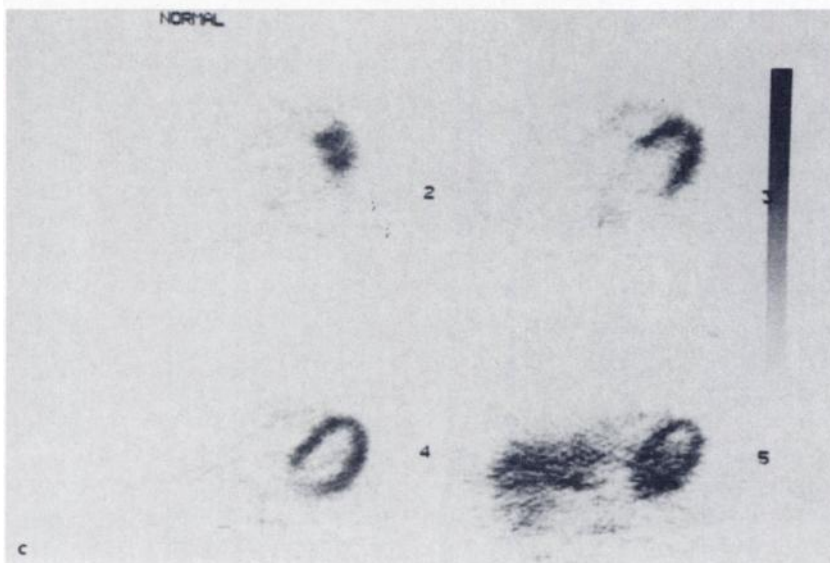
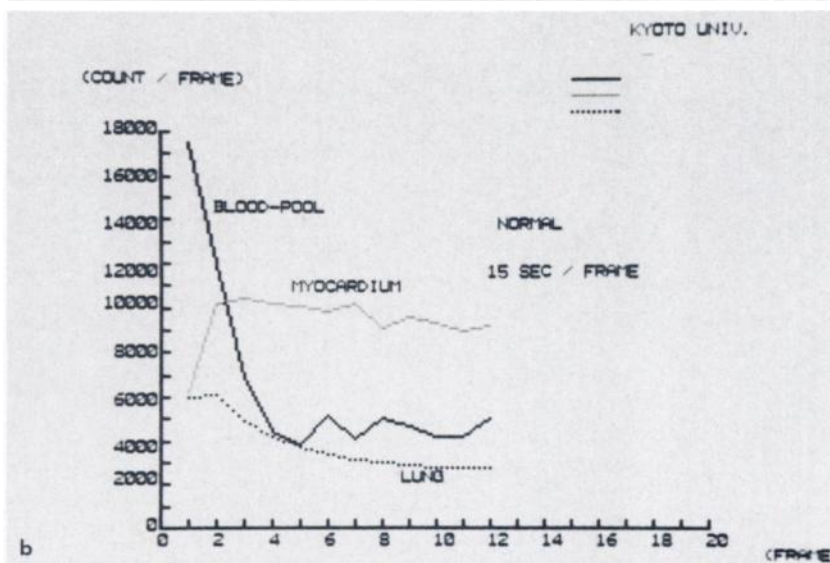
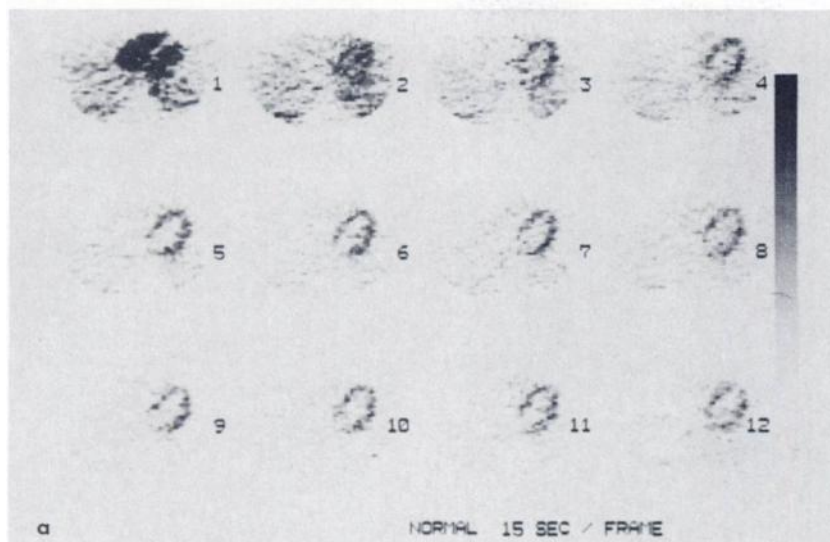


**FIGURE 1**  
 Normal case. a: Serial 15-sec positron CT images; b: Time-activity curves for 3 min; and c: Static myocardial perfusion transverse images from cranial to caudal sections at 16-mm intervals. In dynamic study, blood-pool images of ventricular cavities are obtained at first scan and left ventricular myocardial images are observed from third scan

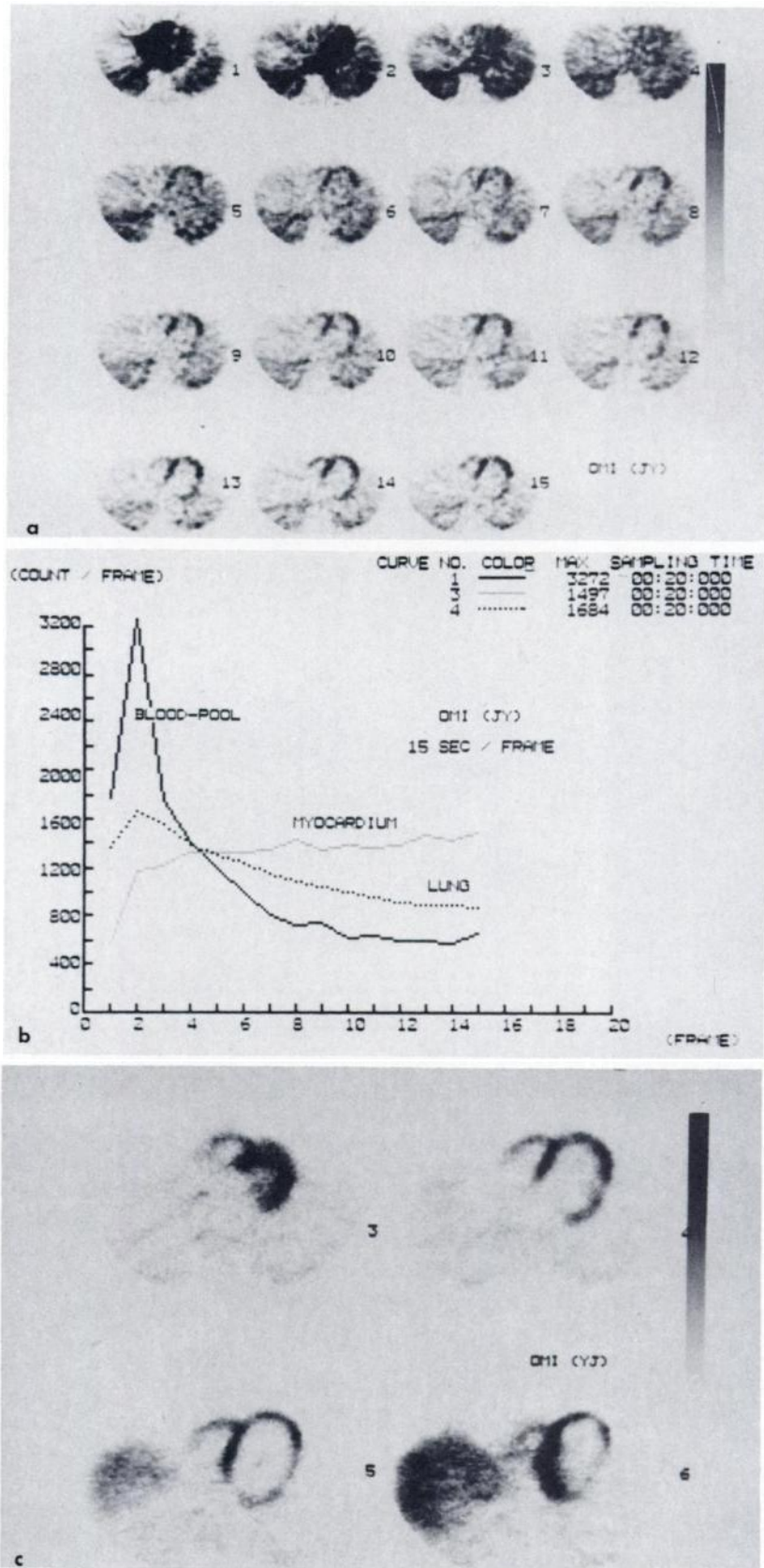


**FIGURE 2**  
 Case with myocardial infarction. a: Serial 15-sec positron CT images; b: Time-activity curves; and c: Static myocardial images. Note prolonged tracer retention in lung in dynamic study

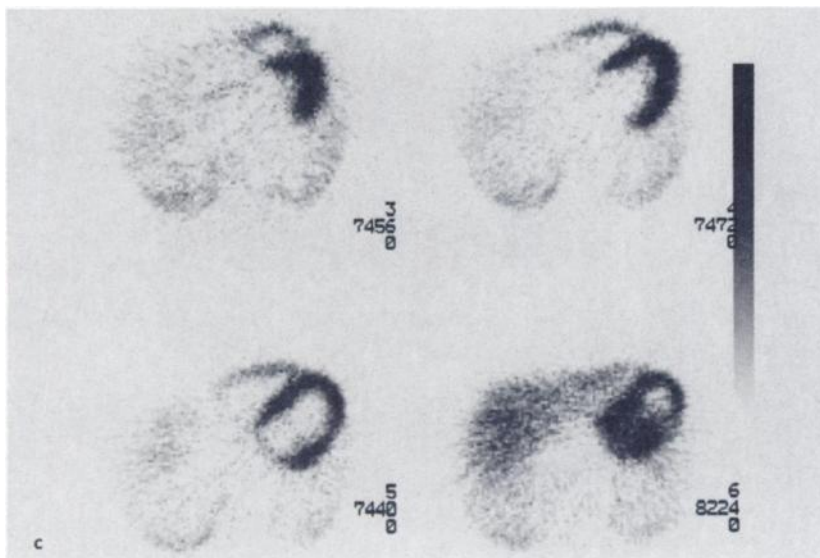
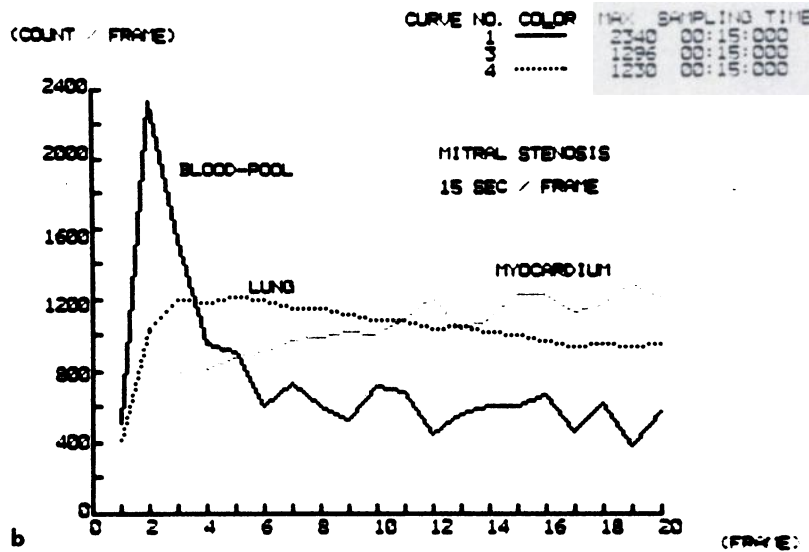
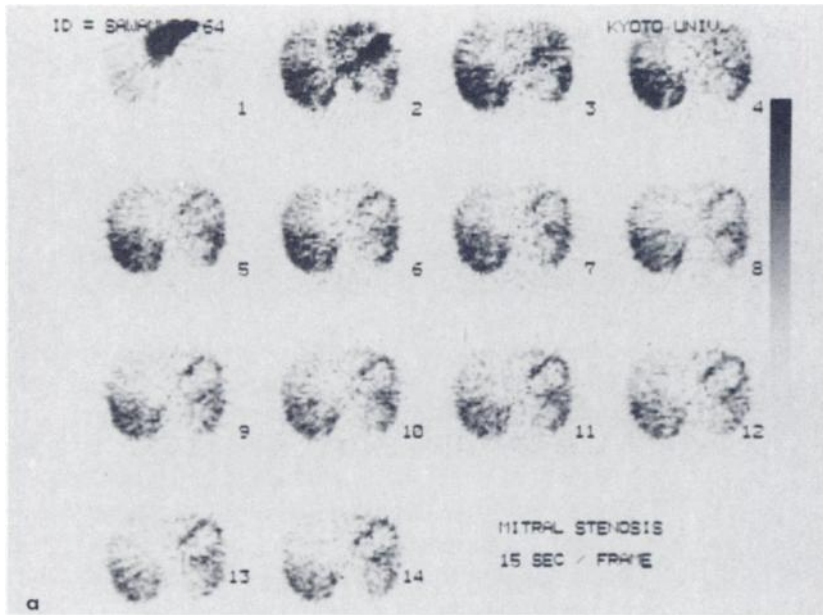


**FIGURE 3**

Case with mitral stenosis. a: Serial 15-sec positron CT images; b: Time-activity curves for 5 min; and c: Static myocardial images. Dynamic study indicates tracer retention in dorsal part of lung with gradual increase in myocardial activity

**TABLE 1**  
Results of Lung- $t_{1/2}$  and Myocardial-Peak Time in 14 Cases (mean  $\pm$  s.d., sec)

Item	Lung- $t_{1/2}$ <sup>*</sup>	Myocardial-peak time <sup>†</sup>
Normal control	52.2 $\pm$ 5.6	60.0 $\pm$ 23.7
Myocardial infarction	165 $\pm$ 76.6 ( $p < 0.05$ )	101.9 $\pm$ 45.3 (N.S.) <sup>‡</sup>
Mitral valve disease	513 $\pm$ 15.0 ( $p < 0.001$ )	202.5 $\pm$ 22.5 ( $p < 0.01$ )

\* Lung- $t_{1/2}$  = half time of the lung washout curve.

† Myocardial-peak time = time to maximal myocardial activity.

‡ N.S. = not significant.

The static images taken 5 min after the injection in this case (Fig. 3c) showed homogeneous activity in the left ventricular myocardium with clear visualization of the right ventricular myocardium.

Table 1 summarizes the results of lung- $t_{1/2}$  and myocardial-peak time in the study of 14 cases. In normal cases, lung- $t_{1/2}$  and myocardial-peak time were 52.5  $\pm$  5.6 sec and 60.6  $\pm$  23.7 sec, respectively (mean  $\pm$  s.d.). Lung- $t_{1/2}$  tended to be longer in cases with MI (165.6  $\pm$  76.6 sec) ( $p < 0.05$ ) and with MVD (315  $\pm$  15.0 sec) ( $p < 0.001$ ). This long pulmonary clearance half-time of [<sup>13</sup>N]ammonia indicates large pulmonary distribution volume, or rather pulmonary congestion. Myocardial-peak time tended to be longer in cases with MVD (202.5  $\pm$  22.5 sec) ( $p < 0.01$ ) and MI (101.9  $\pm$  45.3 sec). Significant positive correlation ( $r = 0.82$ ,  $p < 0.001$ ) was observed between these two parameters (Fig. 4). Thus, long pulmonary transit time of the tracer may result in delayed appearance of the myocardial activity in cases with MI and MVD.

#### Late dynamic scan

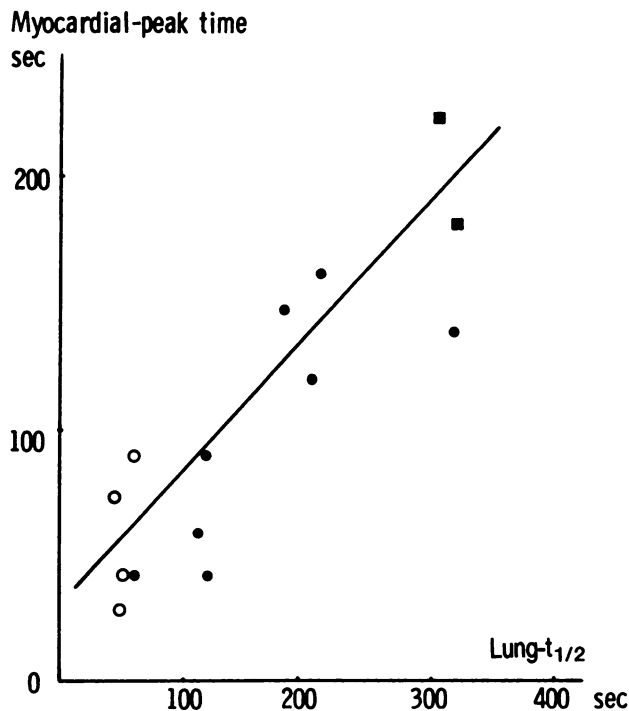
Fig. 5a shows serial 5-min dynamic images in the same MI case as described in Fig. 2. Perfusion defect was noted in apical and posterolateral regions from the first scan. The serial images revealed increased tracer uptake in septal and apical regions, while no increase in lateral region, so that lateral wall defect was more definitely visualized in the late scans. The time-activity curves of regional myocardium for 30 min (Fig. 5b) indicated disparity of the temporal change between in septal-apical regions and in lateral region.

Figure 6 summarized the serial activity changes in each myocardial segment in the study of nine cases. In normal segments, the activity increased in 14–48% of the initial value for 30 min. In infarct segments, on the other

hand, there were two patterns of activity change: activity increase by more than 30% (five segments: 42%) and only a slight increase by less than 13% (six segments: 50%).

#### DISCUSSION

This study validates the applicability of the whole-body multislice PCT for serial dynamic assessment of [<sup>13</sup>N]ammonia distribution in the human myocardium. Our newly constructed whole-body PCT device (Positologica III) has four detector rings providing seven slices simultaneously at 16-mm intervals (10,11), which can cover the whole myocardium with a single scan (12). Thus, it is suitable for various dynamic studies in the heart. For evaluation of the tissue kinetics of metabolic and blood-flow tracers, serial dynamic measurements of myocardial activity concentration are essential in investigating regional myocardial metabolism and blood flow (13,14). However, there have been only a few preliminary reports dealing with multislice dynamic PCT for myocardial imaging (15,16). Our PCT device containing 192 small BGO crystals with the packing ratio of 0.894 in each ring provides high sensitivity of 34.2 and 52.5 kcps/ $\mu$ Ci/ml for in-plane and cross-plane, respectively (10,11). Although these images were not gated, rapid dynamic scan with serial 15-sec sampling



**FIGURE 4**  
Correlation between lung washout rate (lung- $t_{1/2}$ ) and time-to-peak myocardium activity (myocardial-peak time). (O) Normal; (●) Myocardial infarction; (■) Mitral valve disease.  $n = 14$ ;  $y = 0.498x + 30.8$ ;  $r = 0.823$

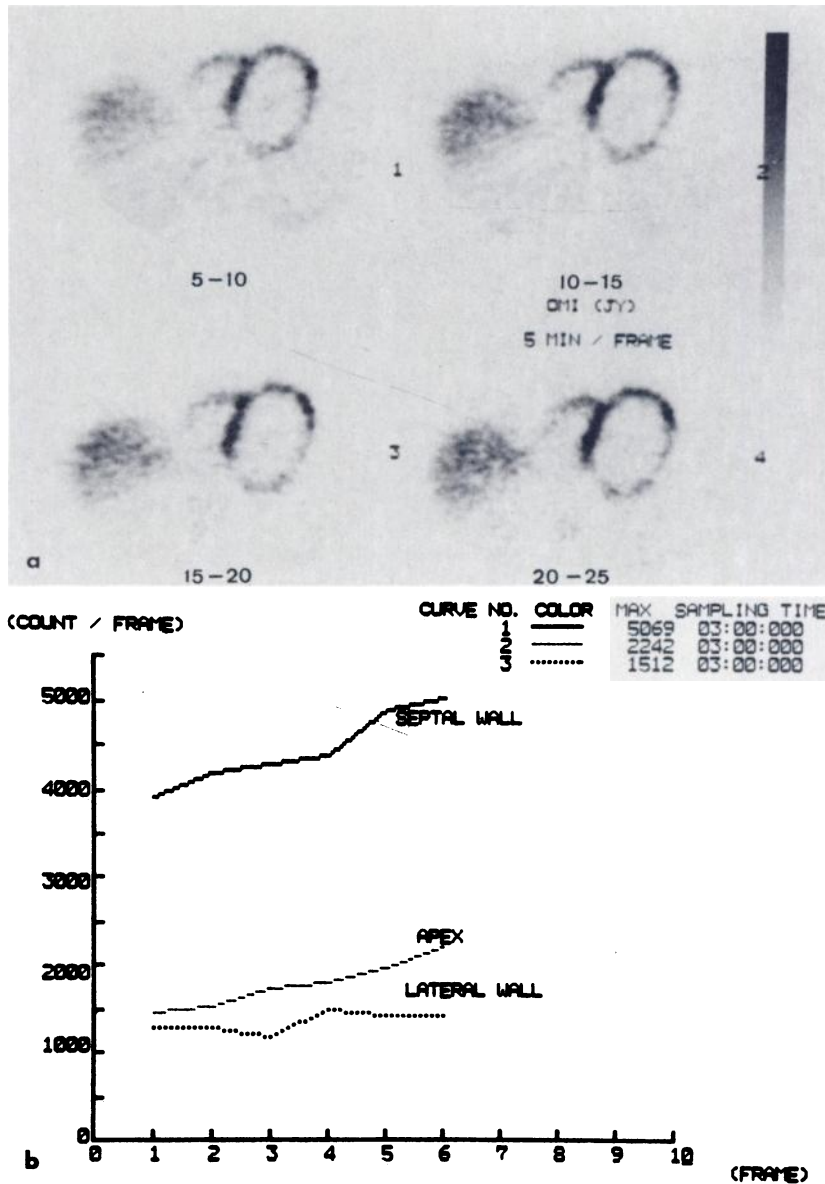


**FIGURE 5**  
Serial 5-min dynamic images from a: 5 min after the injection and b: Time-activity curves of regional myocardium for 30 min in case with MI (same case as in Fig. 2). Increased myocardial activity was observed in septal and apical regions, while no increase in activity was noted in lateral region

is feasible collecting adequate counts for imaging in each scan.

The early rapid dynamic scan in our study permits evaluation of the tracer washout from the blood pool and the lung, and washin into the myocardium. The time-activity curves allow semiquantitative analysis of the tracer kinetics in the lung and the myocardium.

The time-activity curves in cases with MI and MVD revealed prolonged uptake in the lung with delayed appearance of the myocardium, suggesting presence of pulmonary congestion as well as low cardiac output. The dynamic images as well as the static images showed increased lung uptake especially in the dorsal part of the lung in cases with MI and MVD. Thus, regional tracer distribution in the lung can be precisely evaluated by PCT. The tracer in the pulmonary extravascular compartment may then be gradually washed out by pulmo-

nary blood flow and distribute in the whole body, including the brain, the kidney, and the myocardium. Therefore, it is reasonable to show significant positive correlation between tracer washout from the lung ( $\text{lung-t}_{1/2}$ ) and appearance of the myocardium (myocardium-peak time) in our study. The arterial input function should also be considered to evaluate tracer activity in the lung, especially in the study of patients with depressed cardiac function. In this respect, deconvolution of the lung transit time may be helpful. However, arterial input function was not accurate in this study due to poor temporal resolution (15 sec per frame) and large count loss in high count rate.

The late dynamic study for 30 min suggests increase in activity of normal myocardial segments and about half of the infarct segments, while no increase in activity was seen in the remaining infarct segments. In the study of

the late dynamic scan, metabolism of [<sup>13</sup>N]ammonia should be considered. Lockwood et al. (17) reported labeled metabolites of ammonia were detectable in the arterial blood within 3 min after the injection and almost 100% of the <sup>13</sup>N activity was the metabolites by 10 min. Nitrogen-13 ammonia metabolites, mainly [<sup>13</sup>N]glutamine, are formed by skeletal muscle, brain, and other organs (17,18). Nitrogen glutamine is then mainly taken by the liver but also is taken by the myocardium (7). Thus, temporal change in the myocardial activity after 3 min may reflect transfer of [<sup>13</sup>N]ammonia and its metabolites from the blood pool into the myocardium, in addition to myocardial retention in the first transit of [<sup>13</sup>N]ammonia. Considering activity change in the myocardium, quantitative analysis of myocardial blood flow should be carefully performed using metabolized tracer such as [<sup>13</sup>N]ammonia.

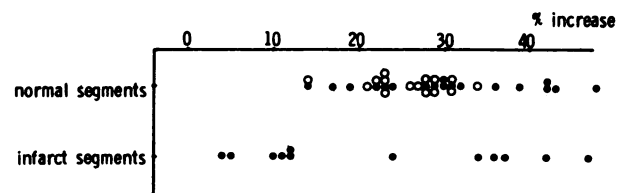


**FIGURE 6**  
Results of serial activity change in regional myocardium for 30 min. (O) Normal; (●) Infarct cases

Nitrogen-13-labeled amino acids could be of potential value for assessment of myocardial metabolism, since amino acids are important intermediates for myocardial protein synthesis and energy metabolism in normal and diseased myocardium (7,19). The residual fraction of [<sup>13</sup>N]glutamine in ischemic myocardium may be about the same (7) or slightly increased (19) than normal myocardium. However, the uptake of [<sup>13</sup>N]glutamine may be severely impaired in myocardial scar without viable tissue. Two different patterns of change in [<sup>13</sup>N]ammonia activity in infarct segments in our study may suggest presence of different metabolic process in infarct segments. Furthermore, increase in myocardial activity in the late dynamic scan may be a potential sign of myocardial viability. Further investigation is necessary in this respect.

In conclusion, our high-sensitivity, multislice PCT permits serial dynamic study of the heart following [<sup>13</sup>N]ammonia injection. The early dynamic scan assessing tracer washout from the lung and washin into the myocardium was valuable for evaluation of pulmonary congestion. The late dynamic scan identified an increase in activity in normal myocardium, while no redistribution was observed in 50% of infarct segments. Thus, these dynamic PCT studies using [<sup>13</sup>N]ammonia should be a valuable adjunct to the static myocardial perfusion imaging for evaluation of various cardiac disorders.

## FOOTNOTE

\* CYPRIS, Model 325, Sumitomo Heavy Industries Ltd., Tokyo, Japan.

## REFERENCES

1. Ter-Pogossian MM: Basic principles of computed axial tomography. *Semin Nucl Med* 7:109-128, 1977
2. Phelps ME, Hoffman EJ, Coleman RE, et al: Tomographic images of blood-pool and perfusion in brain and heart. *J Nucl Med* 17:603-612, 1976
3. Gould KL, Schelbert HR, Phelps ME, et al: Noninvasive assessment of coronary artery stenoses with myocardial perfusion imaging during pharmacologic coronary vasodilatation. V. Detection of 47 percent diameter coronary stenosis with intravenous nitrogen-13 ammonia and emission-computed tomography in intact dogs. *Am J Cardiol* 43:200-208, 1979
4. Schelbert HR, Wisenberg G, Phelps ME, et al: Noninvasive assessment of coronary stenoses by myocardial imaging during pharmacologic coronary casodilation. VI. Detection of coronary artery disease in human beings with intravenous N-13 ammonia and positron computed tomography. *Am J Cardiol* 49:1197-1207, 1982
5. Goldstein RA, Klein MS, Welch MJ, et al: External assessment of myocardial metabolism with C-11 palmitate in vivo. *J Nucl Med* 21:342-348, 1980
6. Phelps ME, Hoffman EJ, Selin C, et al: Investigation of <sup>18</sup>F-2-fluoro-2-deoxyglucose for the measurement of myocardial glucose metabolism. *J Nucl Med* 19:1311-1320, 1978
7. Henze E, Schelbert HR, Barrio JR, et al: Evaluation of myocardial metabolism, with N-13- and C-11-labeled amino acids and positron computed tomography. *J Nucl Med* 23:671-681, 1982
8. Weiss ES, Ahmed SA, Welch MJ, et al: Quantification of infarction in cross sections of canine myocardium in vivo with positron emission transaxial tomography and <sup>11</sup>C-palmitate. *Circulation* 55:66-73, 1977
9. Goodwin PN: Recent developments in instrumentation for emission computed tomography. *Semin Nucl Med* 10:322-334, 1980
10. Takami K, Ueda K, Okajima K, et al: Performance study of whole-body, multislice positron computed tomograph: Positologica II. *IEEE Trans Nucl Sci* NS-30:734-738, 1983
11. Senda M, Tamaki N, Yonekura Y, et al: Performance characteristics of Positologica III: A newly designed whole-body multislice positron computed tomograph. *J Comput Assist Tomogr*: in press
12. Tamaki N, Yonekura Y, Senda M, et al: Comparative study of myocardial perfusion imaging by Tl-201 single-photon ECT and N-13 ammonia positron CT. *J Nucl Med* 25:P6, 1984 (abstr)
13. Schelbert HR, Henze E, Phelps ME, et al: Assessment of regional myocardial ischemia by positron-emission computed tomography. *Am Heart J* 103:588-597, 1982
14. Henze E, Huang SC, Ratib O, et al: Measurements of regional tissue and blood-pool radiotracer concentrations from serial tomographic images of the heart. *J Nucl Med* 24:987-996, 1983
15. Soussaline F, Campagnolo R, Verney B, et al: Physical characterization of a time-of-flight positron emission tomography system for whole-body quantitative studies.

- J Nucl Med* 25:P46, 1984 (abstr)
16. Wong WH, Mullani NA, Phillippe EA, et al: Performance characteristics of the University of Texas TOF-PET-I PET camera. *J Nucl Med* 25:P46, 1984 (abstr)
  17. Lockwood AH, McDonald JM, Reiman RE, et al: The dynamics of ammonia metabolism in man. *J Clin Invest* 63:449-460, 1979
  18. Garber AJ, Karl IE, Kipnis DM: Alanine and glutamine synthesis and release from skeletal muscle II. The precursor role of amino acids in alanine and glutamine synthesis. *J Biol Chem* 251:836-843, 1976
  19. Mudge GH, Mills RM, Taegtmeier H, et al: Alterations in myocardial amino acid metabolism in chronic ischemic heart disease. *J Clin Invest* 58:1186-1192, 1976